AIMS Mathematics, 10(3): 5158–5172.
DOI:10.3934/math.2025237
Received: 19 December 2024
Revised: 26 February 2025
Accepted: 04 March 2025
Published: 07 March 2025

https://www.aimspress.com/journal/Math

Research article

Bifurcations and exact solutions of generalized nonlinear Schrödinger equation

Qian Zhang[1] **and Ai Ke**[2,*]

[1] School of Mathematics and Physics, Southwest University of Science and Technology, Mianyang 621010, Sichuan, China

[2] School of Mathematical Sciences, Zhejiang Normal University, Jinhua 321004, Zhejiang, China

* **Correspondence:** Email: aike_math@zjnu.edu.cn.

Abstract: To find the exact explicit solutions of the generalized nonlinear Schrödinger equation, we first give the corresponding differential system for the amplitude component, which constitutes a planar dynamical system featuring a singular straight line. By analyzing its corresponding traveling wave system, we can derive the dynamical behavior of the amplitude component and give the corresponding phase portraits. Under different parameter conditions, we obtain exact explicit solitary wave solutions, periodic wave solutions, as well as peakons and periodic peakons. By comparing our results with previous studies on the generalized nonlinear Schrödinger equation, we correct the error regarding the first integral and present accurate solutions to the equation.

Keywords: solitary wave; periodic wave; peakon; periodic peakon; traveling wave system
Mathematics Subject Classification: 34C23, 34C37, 74J30

1. Introduction

We consider the following nonlinear partial differential equation:

$$iQ_t + Q_{xx} + \alpha Q + \beta|Q|^n Q + \gamma|Q|^{2n} Q + \delta|Q|^{3n} Q + \lambda|Q|^{4n} Q = 0, \tag{1.1}$$

where $Q(x,t)$ is a complex function representing the wave amplitude, x is the coordinate, t is the time, n is a rational number indicating the nonlinearity order, and $\alpha, \beta, \gamma, \delta, \lambda$ are related to the dispersion and nonlinearity of the medium. We consider the generalized nonlinear Schrödinger equation (1.1) due to its broad applicability in describing pulse propagation in nonlinear optical fibers. This equation extends the standard nonlinear Schrödinger equation by incorporating higher-order nonlinear terms, providing a more accurate model for complex optical systems (see [11–13,26] for example). There are

many studies about the generalized nonlinear Schrödinger equation; see references in [5, 6, 10, 17, 19]. Elsonbaty et al. [5] considered a newly generalized nonlinear Schrödinger equation with a triple refractive index and non-local nonlinearity. In order to obtain optical solitons for a specific case of this innovative model, they employed the improved modified extended tanh function method. And they derived various solutions, including bright solitons, dark solitons, singular solitons, singular periodic solutions, trigonometric solutions, and hyperbolic solutions. Wang and Yang studied [19] a generalized nonlinear Schrödinger equation by constructing the modified generalized Darboux transformation. They analyzed the type-I, type-II, and type-III degenerate solitons for the equation by some semirational solutions. In particular, letting $n = 2, \beta \neq 0, \alpha = \gamma = \delta = \lambda = 0$, Eq (1.1) becomes the famous nonlinear Schrödinger equation. In [11], the author proposed a more generalized equation for describing pulse propagation in optical fiber in the form

$$iQ_t + Q_{xx} + \alpha Q + \beta Q|Q|^{2m-2n} + \gamma Q|Q|^{2m-n} + \delta Q|Q|^{2m+n} + \lambda Q|Q|^{2m+2n} = 0, \tag{1.2}$$

where m, n are rational numbers.

In fact, (1.1) is a special case of (1.2) for the case $m = n$. In addition, letting $m = 0$, (1.2) can be written as follows:

$$iQ_t + Q_{xx} + \alpha Q + \beta Q|Q|^{-2n} + \gamma Q|Q|^{-n} + \delta Q|Q|^{n} + \lambda Q|Q|^{2n} = 0, \tag{1.3}$$

which was introduced in paper [9] and has been widely investigated. However, Eq (1.3) cannot be implemented in practice according to physicists on account of the negative degree terms. Therefore, Eq (1.2) for $m \neq 0$ is better than Eq (1.1) for describing the propagation of various types of pulses in an optical fiber. In paper [11], some solutions of Eq (1.2) for two cases, $m = n$ and $m = 2n$, were obtained by applying the variable transformation method.

In addition, Eq (1) generalizes several equations describing propagation pulses in nonlinear optics (see [1, 2, 7, 8, 20, 22] for example). In [10], the author derived the implicit solitary wave solutions of (1.1) through transformations of variables. However, it is worth noting that there may be some potential errors affecting the correctness of the results in [10].

We hope to find solutions to Eq (1.1) as follows:

$$Q(x, t) = \phi(\xi)e^{i(\kappa x - \omega t)}, \quad \xi = x - vt, \tag{1.4}$$

where κ and ω represent real-valued constants, ξ denotes the wave variable, and $\phi(\xi)$ stands for the amplitude component. Substituting (1.4) into (1.1), dividing by the complex exponential function $e^{i(\kappa x - \omega t)}$, and separating the real and imaginary parts, one obtains two ordinary differential equations

$$\phi'' + (-\kappa^2 + \alpha + \omega)\phi + \beta\phi^{n+1} + \gamma\phi^{2n+1} + \delta\phi^{3n+1} + \lambda\phi^{4n+1} = 0, \tag{1.5}$$

and

$$(2\kappa - v)\phi' = 0, \tag{1.6}$$

where $'$ represents differentiation with respect to ξ. Obviously, (1.6) implies that $v = 2\kappa$.

Let $b = -\kappa^2 + \alpha + \omega$. Then (1.5) is equivalent to the following system:

$$\frac{d\phi}{d\xi} = y, \quad \frac{dy}{d\xi} = -\left(b\phi + \beta\phi^{n+1} + \gamma\phi^{2n+1} + \delta\phi^{3n+1} + \lambda\phi^{4n+1}\right),$$

which has a first integral of the form

$$H_0(\phi, y) = y^2 + b\phi^2 + \frac{2\beta}{n+2}\phi^{n+2} + \frac{\gamma}{n+1}\phi^{2n+2} + \frac{2\delta}{3n+2}\phi^{3n+2} + \frac{\lambda}{2n+1}\phi^{4n+2} = h. \tag{1.7}$$

According to [4, 21, 24], we can make the following transformation:

$$\phi = \psi^{-\frac{1}{n}}. \tag{1.8}$$

Noting

$$\phi'' = \frac{1}{n}\left(\frac{1}{n} + 1\right)\psi^{-\frac{1}{n}-2}(\psi')^2 - \frac{1}{n}\psi^{-\frac{1}{n}-1}\psi'', \tag{1.9}$$

and substituting (1.8) and (1.9) into (1.5), then one has

$$\psi^3\psi'' - n(b\psi^4 + \beta\psi^3 + \gamma\psi^2 + \delta\psi + \lambda) - \left(1 + \frac{1}{n}\right)\psi^2(\psi')^2 = 0. \tag{1.10}$$

Equation (1.10) is equivalent to the planar dynamical system as follows:

$$\frac{d\psi}{d\xi} = y, \quad \frac{dy}{d\xi} = \frac{\left(1 + \frac{1}{n}\right)\psi^2 y^2 + n(b\psi^4 + \beta\psi^3 + \gamma\psi^2 + \delta\psi + \lambda)}{\psi^3}, \tag{1.11}$$

where ψ represents the transformed amplitude component, ξ is the wave variable, and n is the nonlinearity order. It is easy to see that system (1.11) has a first integral of the form

$$H(\psi, y) = y^2\psi^{-\frac{2n+2}{n}} + n^2\psi^{-\frac{4n+2}{n}}\left(\frac{\lambda}{2n+1} + \frac{2\delta}{3n+2}\psi + \frac{\gamma}{n+1}\psi^2 + \frac{2\beta}{n+2}\psi^3 + b\psi^4\right) = h, \tag{1.12}$$

for $n \neq -\frac{1}{2}, -\frac{2}{3}, -1, -2$. If $n = -\frac{1}{2}, -\frac{2}{3}, -1, -2$, then $H(\psi, y)$ contains a term of $\ln(\cdot)$; we omit them.

Remark 1. *In [10], the author did not derive system (1.11). If we only consider $H_0(\phi, y) = h$ given by (1.7), then the transformation (1.8) makes (1.7) become*

$$\psi^2(\psi')^2 + n^2\left(b\psi^4 + \frac{2\beta}{n+2}\psi^3 + \frac{\gamma}{n+1}\psi^2 + \frac{2\delta}{3n+2}\psi + \frac{\lambda}{2n+1} - h\psi^{4+\frac{2}{n}}\right) = 0. \tag{1.13}$$

Clearly, (1.13) is different from (1.12).

The author of [10] supposed that the first integral of the equation derived by his transformation was

$$(\psi')^2 + (-\kappa^2 + \alpha + \omega)n^2\psi^4 + \frac{2n^2\beta}{n+2}\psi^3 + \frac{n^2\gamma}{n+1}\psi^2 + \frac{2n^2\delta}{3n+2}\psi + \frac{n^2\lambda}{2n+1} = 0, \tag{1.14}$$

i.e., the formula (12) on page 2 of his paper. As we mentioned above in (1.12), this first integral is incorrect for the Eq (1.11). Therefore, the results in his paper [10] need to be corrected. Actually, they did not derive and study the traveling wave system (1.11). Similar mistakes appeared in Rogers et al. [18] and Zayed et al. [23]. Their results had been corrected by Zhou et al. [27].

We need to say that for an integrable planar differential system, if we make a variable transformation like (1.8), we must derive a new equation with respect to the new variable, and we have to find the new first integral.

System (1.11) is a six-parameter system that relies on the parameter set $(b, n, \beta, \gamma, \delta, \lambda)$. It has very abundant dynamical behavior. Furthermore, as defined in [14] and [15], it is classified as the first kind of singular traveling wave system, which has the singular straight line $\psi = 0$. In recent years, many researchers have employed the dynamical systems approach to explore the dynamical behaviors of solutions for the first kind of singular systems and to provide possible parametric representations of solutions (see [16, 25] for example).

In this paper, we first assume that $\delta = \lambda = 0$, $n = -\frac{1}{3}$, and $n = 2$. We analyze the bifurcations of phase portraits of system (1.11) when there exist two real zeros of $f(\psi) = b\psi^2 + \beta\psi + \gamma$. Then, we calculate all possible exact explicit peakons, periodic peakons, smooth periodic solutions, as well as homoclinic orbits of system (1.11). The exact parametric representations of these solutions are presented.

The article is organized as follows: In Section 2, we analyze the bifurcations of phase portraits for (1.11). In Sections 3 and 4, we derive all possible exact explicit parametric representations for some bounded solutions of (1.11). In Section 5, we state the main results of this paper.

2. The bifurcations of phase portraits of (1.11) with $\delta = \lambda = 0$

When $\delta = \lambda = 0$, system (1.11) is reduced to

$$\frac{d\psi}{d\xi} = y, \quad \frac{dy}{d\xi} = \frac{\left(1 + \frac{1}{n}\right) y^2 + n(b\psi^2 + \beta\psi + \gamma)}{\psi}. \tag{2.1}$$

The associated system of (2.1) can be written as

$$\frac{d\psi}{d\zeta} = y\psi, \quad \frac{dy}{d\zeta} = \left(1 + \frac{1}{n}\right) y^2 + n(b\psi^2 + \beta\psi + \gamma), \tag{2.2}$$

where $d\xi = \psi d\zeta$.

Suppose that $\Delta = \beta^2 - 4b\gamma \geq 0$. Then (2.1) has two equilibrium points $E_1(\psi_1, 0)$ and $E_2(\psi_2, 0)$, where $\psi_{1,2} = \frac{1}{2b}(-\beta \mp \sqrt{\Delta})$ with $\psi_1 < \psi_2$.

When $(n + 1)\gamma < 0$, we have $Y_s = \frac{-n^2\gamma}{n+1} > 0$. Then on the straight line $\psi = 0$, system (2.2) has two equilibrium points $S_{\mp}\left(0, \mp\sqrt{Y_s}\right)$.

Let $M(\psi_j, 0)$ represent the coefficient matrix for the linearized system of system (2.2), at the point $E_j(\psi_j, 0)$, $j = 1, 2$. Let $J(\cdot, \cdot)$ be their Jacobian determinants. Then

$$J(\psi_j, 0) = -n(2b\psi_j + \beta)\psi_j, \quad j = 1, 2,$$

$$J\left(0, \mp\sqrt{Y_s}\right) = 2\left(1 + \frac{1}{n}\right) Y_s.$$

By the theory of planar dynamical systems, for an equilibrium point of a planar integrable system, if $J < 0$, then the equilibrium point is a saddle point; if $J > 0$ and $(\text{Trace}(M(\psi_j, 0)))^2 - 4J(\psi_j, 0) < 0$, then it is a center point; if $J > 0$ and $(\text{Trace}(M(\psi_j, 0)))^2 - 4J(\psi_j, 0) > 0$, then it is a node; if $J = 0$ and the Poincaré index of the equilibrium point is 0, then it is a cusp.

For H defined by (1.12), we write that $h_j = H(\psi_j, 0)$, $j = 1, 2$ and $h_s = H(0, \sqrt{Y_s})$.

As two examples, we take $n = -\frac{1}{3}$ and $n = 2$. Utilizing the aforementioned information for qualitative analysis, we obtain the bifurcations of phase portraits of system (2.1), which are displayed in Figures 1 and 2.

2.1. Assume that $n = -\frac{1}{3}$ and $\beta > 0, \gamma < 0$ are two fixed parameters

In this case, we know that $Y_s > 0$ and $J(0, \mp\sqrt{Y_s}) < 0$. Therefore, the equilibrium points $S_\mp$ are two saddle points. Let $b_p := \frac{\beta^2}{4\gamma}$. Then the function $F(\psi) = b\psi^2 + \beta\psi + \gamma$ has two different real zeros for $b_p < b < 0$ or $b > 0$, which implies system (2.1) has two equilibrium points. Based on the above results, by varying b, we get the bifurcations of phase portraits of (2.1), which are displayed in Figure 1. In the case of $\gamma > 0$, we do not consider it here.

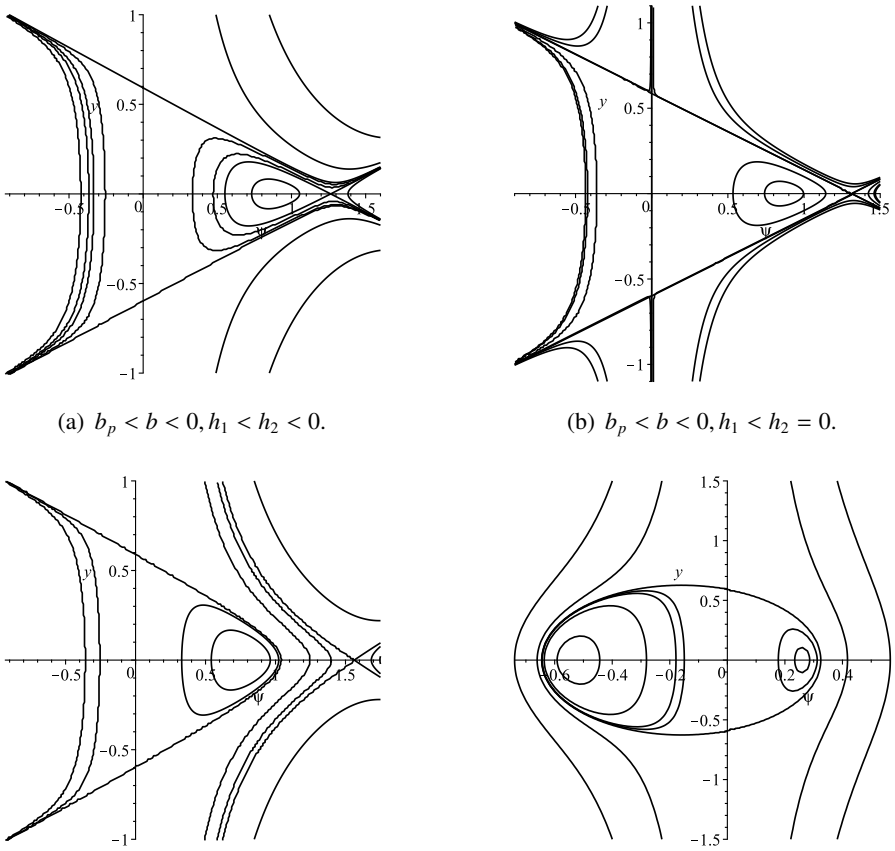

(a) $b_p < b < 0, h_1 < h_2 < 0$.

(b) $b_p < b < 0, h_1 < h_2 = 0$.

(c) $b_p < b < 0, h_1 < 0 < h_2$.

(d) $b > 0, h_1 < h_2 < 0$.

Figure 1. The bifurcations of phase portraits of system (2.1) in the case $n = -\frac{1}{3}$. This figure illustrates the transition between different dynamical behaviors, such as periodic and solitary wave solutions, as the parameter b varies. The bifurcation points correspond to critical changes in the system's stability and wave propagation characteristics.

2.2. Assume that $n = 2$ and $\beta > 0$ is a fixed parameter

When $\gamma < 0$, noting that $Y_s > 0$, $J(0, \mp\sqrt{Y_s}) > 0$, and $(\text{Trace}(M(0, \mp\sqrt{Y_s})))^2 - 4J(0, \mp\sqrt{Y_s}) > 0$, one finds that $S_\mp$ are two node points. When $\gamma > 0$, there are no equilibrium points on the singular straight line $\psi = 0$ because $Y_s < 0$. By varying b such that $\Delta > 0$, i.e., $b_p < b < 0$ or $b > 0$ when $\gamma < 0$ ($0 < b < b_p$ or $b < 0$ when $\gamma > 0$, respectively), we obtain the bifurcations of phase portraits of (2.1), which are displayed in Figure 2.

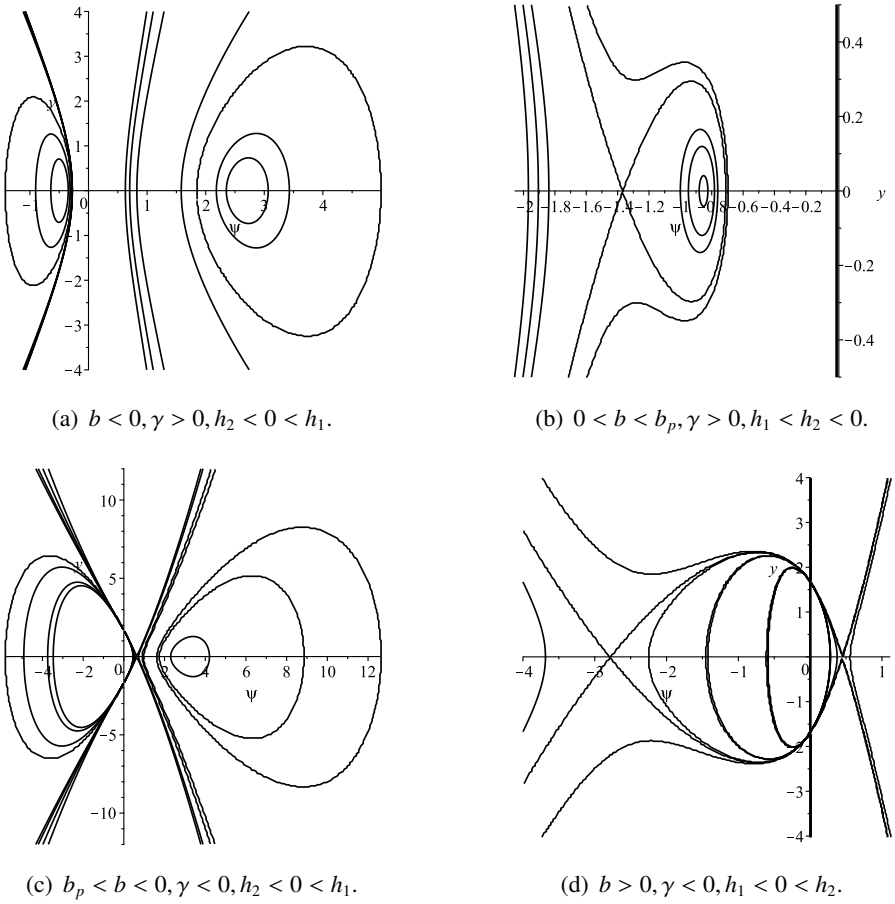

(a) $b < 0, \gamma > 0, h_2 < 0 < h_1$. (b) $0 < b < b_p, \gamma > 0, h_1 < h_2 < 0$.

(c) $b_p < b < 0, \gamma < 0, h_2 < 0 < h_1$. (d) $b > 0, \gamma < 0, h_1 < 0 < h_2$.

Figure 2. The bifurcations of phase portraits of system (2.1) in the case $n = 2$.

3. The exact parametric representations of some bounded solutions given by (2.1) in Figure 1

In this section, some parametric representations for the bounded orbits in Figure 1 are derived. In this case, we have the parameter condition $n = -\frac{1}{3}$ and $\beta > 0, \gamma < 0$. We see from (1.12) that $y^2 = \frac{h}{\psi^4} - \frac{1}{9}(b\psi^2 + \frac{6}{5}\beta\psi + \frac{3}{2}\gamma)$. By using the first equation of (2.1), one has

$$\xi = \int_{\psi_0}^{\psi} \frac{\psi^2 d\psi}{\sqrt{\left|h - \frac{1}{9}\psi^4\left(b\psi^2 + \frac{6}{5}\beta\psi + \frac{3}{2}\gamma\right)\right|}}. \tag{3.1}$$

For some orbits shown in Figure 1, if the integral of the right-hand side of (3.1) can be calculated, then we can obtain their parametric representations.

3.1. The case of $b > 0, h_1 < h_2 < 0$ illustrated in Figure 1(d)

Corresponding to the closed orbit defined by $H(\psi, y) = 0$ in Figure 1(d), enclosing the equilibrium points $E_j(\psi_j, 0)$, $j = 1, 2$, and passing through the singular straight line $\psi = 0$, (3.1) can be written as

$$\frac{\sqrt{b}}{3}\xi = \int_0^{\psi} \frac{d\psi}{\sqrt{(\psi_M - \psi)(\psi - \psi_m)}},$$

where ψ_M, ψ_m are determined by

$$\left|\psi^2 + \frac{6\beta}{5b}\psi + \frac{3\gamma}{2b}\right| = (\psi_M - \psi)(\psi - \psi_m)$$

with $\psi_m < \psi < \psi_M$. Thus, it follows that the parametric representation of a periodic solution (see Figure 3(a)):

$$\psi(\xi) = \frac{1}{2}\left[(\psi_M - \psi_m)\sin\left(\frac{\sqrt{b}}{3}\xi - \xi_{01}\right) + (\psi_M - \psi_m)\right], \tag{3.2}$$

where $\xi_{01} = \arcsin\left(\frac{\psi_M+\psi_m}{\psi_M-\psi_m}\right)$.

3.2. The case of $b_p < b < 0, h_1 < 0 < h_2$ illustrated in Figure 1(c)

Corresponding to the arch orbit defined by $H(\psi, y) = 0$ in Figure 1(c), enclosing the equilibrium point $E_2(\psi_2, 0)$, (3.1) can be represented as

$$\frac{\sqrt{|b|}}{3}\xi = \int_{\psi}^{\psi_M} \frac{d\psi}{\sqrt{(\psi_L - \psi)(\psi_M - \psi)}},$$

where ψ_M, ψ_L are determined by

$$\left|\psi^2 + \frac{6\beta}{5b}\psi + \frac{3\gamma}{2b}\right| = (\psi_L - \psi)(\psi_M - \psi)$$

with $\psi < \psi_M < \psi_L$. Thus, we obtain the following parametric representation of a periodic peakon solution (see Figure 3(b)):

$$\psi(\xi) = \frac{1}{2}\left[-(\psi_L - \psi_M)\cosh\left(\frac{\sqrt{|b|}}{3}\xi\right) + (\psi_L + \psi_M)\right], \quad \xi \in (-\xi_{02}, \xi_{02}), \tag{3.3}$$

where $\xi_{02} = \frac{3}{\sqrt{|b|}}\cosh^{-1}\left(\frac{\psi_L+\psi_M}{\psi_L-\psi_M}\right)$.

3.3. The case of $b_p < b < 0, h_1 < h_2 = 0$ illustrated in Figure 1(b)

Corresponding to the triangle orbit defined by $H(\psi, y) = 0$ in Figure 1(b), enclosing the singular point $E_1(\psi_1, 0)$, (3.1) can be represented as

$$\frac{\sqrt{|b|}}{3}\xi = \int_{0}^{\psi} \frac{d\psi}{\psi_2 - \psi}.$$

It generates the parametric representation of an anti-peakon solution (see Figure 3(c)) as follows:

$$\psi(\xi) = \psi_2\left(1 - e^{-\frac{\sqrt{|b|}}{3}|\xi|}\right). \tag{3.4}$$

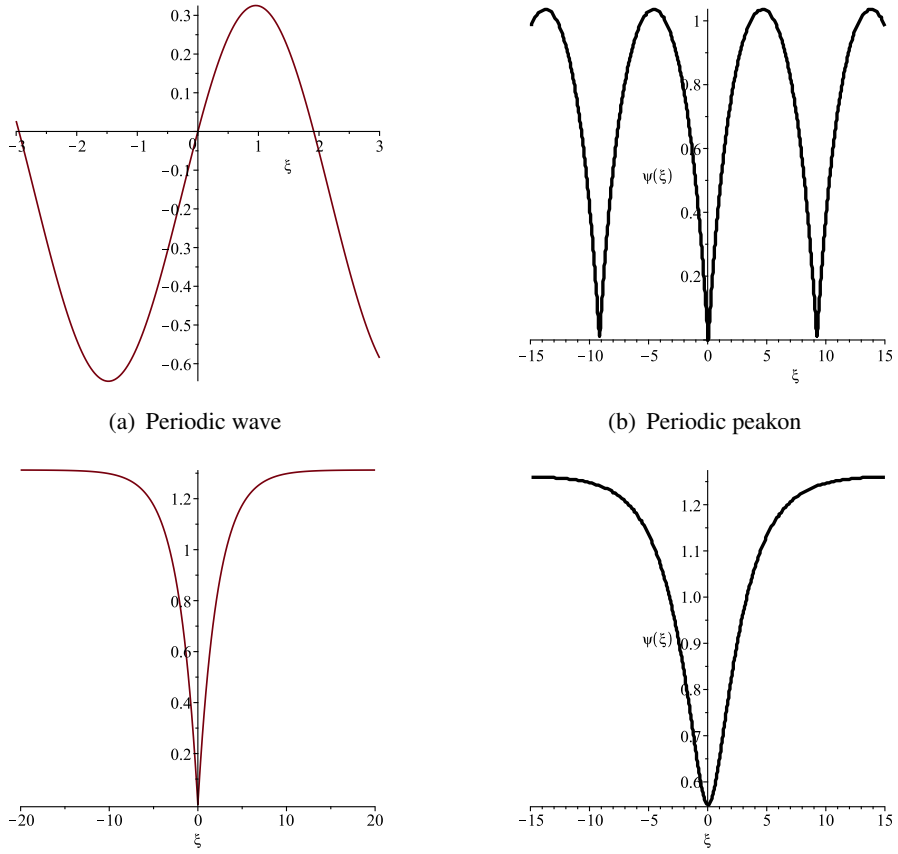

(a) Periodic wave (b) Periodic peakon

(c) Anti-Peakon (d) Solitary wave

Figure 3. The wave profiles of $\psi(\xi)$ of system (2.1) in Figure 1.

3.4. The case of $b_p < b < 0, h_1 < h_2 < 0$ illustrated in Figure 1(a)

Corresponding to the homoclinic orbits to the singular point $E_2(\psi_2, 0)$ defined by $H(\psi, y) = h_2$ in Figure 1(a), enclosing the singular point $E_1(\psi_1, 0)$, (3.1) can be represented as

$$\frac{\sqrt{|b|}}{3}\xi = \int_{\psi_m}^{\psi} \frac{\psi^2 d\psi}{(\psi_2 - \psi)\sqrt{(\psi - \psi_m)(\psi - \psi_l)[(\psi - b_1)^2 + a_1^2]}},$$

where ψ_m, ϕ_l, b_1, a_1 are determined by

$$\left|\frac{9h_2}{b} - \psi^4\left(\psi^2 + \frac{6\beta}{5b}\psi + \frac{3}{2b}r\right)\right| = (\psi_2 - \psi)\sqrt{(\psi - \psi_m)(\psi - \psi_l)[(\psi - b_1)^2 + a_1^2]}$$

with $\psi_l < \psi_m < \psi < \psi_2$. It generates the parametric representation of a homoclinic orbit (solitary wave) as follows (see Figure 3(d))

$$\begin{aligned} \psi(\chi) &= \tfrac{\psi_l A_1 - \psi_m B_1 - (\psi_m B_1 + \psi_l A_1)\mathrm{cn}(\chi,k)}{(A_1 - B_1) - (A_1 + B_1)\mathrm{cn}(\chi,k)}, \quad \chi \in (-\chi_{01}, \chi_{01}), \\ \xi(\chi) &= \tfrac{3}{\sqrt{|b|}}\left[-g\psi_2\chi + \int_{\psi_m}^{\psi} \tfrac{\psi d\psi}{\sqrt{(\psi-\psi_m)(\psi-\psi_l)[(\psi-b_1)^2+a_1^2]}}\right. \\ &\quad \left. + \psi_2^2 \int_{\psi_m}^{\psi} \tfrac{d\psi}{(\psi_2-\psi)\sqrt{(\psi-\psi_m)(\psi-\psi_l)[(\psi-b_1)^2+a_1^2]}}\right], \end{aligned} \tag{3.5}$$

where

$$A_1^2 = (\psi_m - b_1)^2 + a_1^2, \quad B_1^2 = (\psi_l - b_1)^2 + a_1^2, \quad k^2 = \frac{(A_1 + B_1)^2 - (\psi_m - \psi_l)^2}{4A_1B_1},$$

$$g = \frac{1}{\sqrt{A_1B_1}}, \quad \chi_{01} = \mathrm{cn}^{-1}\left(\frac{\psi_2(A_1 - B_1) - (\psi_l A_1 - \psi_m B_1)}{\psi_2(A_1 + B_1) - (\psi_m B_1 + \psi_l A_1)}\right),$$

$\mathrm{sn}(\cdot, k), \mathrm{cn}(\cdot, k), \mathrm{dn}(\cdot, k)$ are the Jacobian elliptic functions (see Byrd and Fridman [3]). In the right hand of $\xi(\chi)$, the formulas of two integrals are too longer; we omit them.

4. The exact parametric representations of all bounded solutions given by (2.1) in Figure 2

In this section, parametric representations of all bounded orbits in Figure 2 are derived. In this case, we have the parameter conditions: $n = 2$ and $\beta > 0, \beta^2 > 4b\gamma$. We see from (1.12) that $y^2 = h\psi^3 - 4(b\psi^2 + \frac{1}{2}\beta\psi + \frac{1}{3}\gamma)$. By using the first equation of (2.1), we have

$$\xi = \int_{\psi_0}^{\psi} \frac{d\psi}{\sqrt{\left|h\psi^3 - 4(b\psi^2 + \frac{1}{2}\beta\psi + \frac{1}{3}\gamma)\right|}}. \tag{4.1}$$

4.1. The case of $b < 0, \gamma > 0, h_2 < 0 < h_1$ illustrated in Figure 2(a)

(i) Corresponding to the periodic orbit family defined by $H(\psi, y) = h, h \in (h_2, 0)$ in Figure 2(a), enclosing the singular point $E_2(\psi_2, 0)$, (4.1) can be represented as

$$\sqrt{|h|}\xi = \int_{\psi_b}^{\psi} \frac{d\psi}{\sqrt{(\psi_a - \psi)(\psi - \psi_b)(\psi - \psi_c)}},$$

where ψ_a, ψ_b, ψ_c are determined by

$$\left|\psi^3 - \frac{4}{h}\left(b\psi^2 + \frac{1}{2}\beta\psi + \frac{1}{3}\gamma\right)\right| = (\psi_a - \psi)(\psi - \psi_b)(\psi - \psi_c), \quad h \in (h_2, 0)$$

with $\psi_a > \psi > \psi_b > \psi_c$. It follows that the parametric representation of the right family of periodic orbits

$$\psi(\xi) = \psi_c + \frac{\psi_b - \psi_c}{\mathrm{dn}^2\left(\frac{1}{2}\sqrt{|h|(\psi_a - \psi_c)}\xi, k\right)}, \tag{4.2}$$

where

$$k^2 = \frac{\psi_a - \psi_c}{\psi_a - \psi_c}.$$

(ii) Corresponding to the periodic orbit family given by $H(\psi, y) = h, h \in (0, h_1)$ in Figure 2(a), enclosing the singular point $E_1(\psi_1, 0)$, (4.1) can be represented as

$$\sqrt{h}\xi = \int_{\psi_c}^{\psi} \frac{d\psi}{\sqrt{(\psi_a - \psi)(\psi_b - \psi)(\psi - \psi_c)}},$$

where ψ_a, ψ_b, ψ_c are determined by

$$\left|\psi^3 - \frac{4}{h}\left(b\psi^2 + \frac{1}{2}\beta\psi + \frac{1}{3}\gamma\right)\right| = (\psi_a - \psi)(\psi - \psi_b)(\psi - \psi_c), \quad h \in (0, h_1)$$

with $\psi_a > \psi_b > \psi > \psi_c$. It follows that the parametric representation of the left family of periodic orbits

$$\psi(\xi) = \psi_c + (\psi_b - \psi_c)\mathrm{sn}^2\left(\frac{1}{2}\sqrt{h(\psi_a - \psi_c)}\xi, k\right), \tag{4.3}$$

where

$$k^2 = \frac{\psi_b - \psi_c}{\psi_a - \psi_c}.$$

4.2. The case of $b > 0, \gamma > 0, h_1 < h_2 < 0$ illustrated in Figure 2(b)

(i) Corresponding to the periodic orbit family given by $H(\psi, y) = h, h \in (h_1, h_2)$ in Figure 2(b), enclosing the singular point $E_2(\psi_2, 0)$, it has the same parametric representation as (4.2).

(ii) Corresponding to the homoclinic orbit to the singular point $E_1(\psi_1, 0)$ given by $H(\psi, y) = h_1$ in Figure 2(b), enclosing the singular point $E_2(\psi_2, 0)$, (4.1) can be represented as

$$\sqrt{|h_1|}\xi = \int_{\psi}^{\psi_M} \frac{d\psi}{(\psi - \psi_1)\sqrt{\psi_M - \psi}},$$

where ψ_M is determined by

$$\left|\psi^3 - \frac{4}{h_1}\left(b\psi^2 + \frac{1}{2}\beta\psi + \frac{1}{3}\gamma\right)\right| = (\psi - \psi_1)\sqrt{\psi_M - \psi},$$

with $\psi_1 < \psi < \psi_M$. Thus, we have the following solitary wave solution:

$$\psi(\xi) = \psi_1 + (\psi_M - \psi_1)\mathrm{sech}^2\left(\frac{1}{2}\sqrt{|h_1|(\psi_M - \psi_1)}\xi\right). \tag{4.4}$$

4.3. The case of $b < 0, \gamma < 0, h_2 < 0 < h_1$ illustrated in Figure 2(c)

In this case the points $S_{\mp}$ are node points of system (2.2). Now, the changes of the level curves given by $H(\psi, y) = h$ are shown in Figure 4.

(i) Corresponding to the periodic orbit family defined by $H(\psi, y) = h, h \in (h_2, 0)$ in Figure 4(a), enclosing the singular point $E_2(\psi_2, 0)$, it has the same parametric representation as (4.2).

(ii) Corresponding to the periodic orbit family given by $H(\psi, y) = h, h \in (0, h_1)$ in Figure 4(c), passing through the singular straight line $\psi = 0$ at $S_{\mp}$, it has the same parametric representation as (4.3).

(iii) Corresponding to the homoclinic orbit to the singular $E_1(\psi_1, 0)$ given by $H(\psi, y) = h_1$ in Figure 4(d), passing through the singular straight line $\psi = 0$ at $S_{\mp}$, now, (4.1) can be written as

$$\sqrt{h_1}\xi = \int_{\psi_m}^{\psi} \frac{d\psi}{(\psi_1 - \psi)\sqrt{\psi - \psi_m}},$$

where ψ_m is determined by

$$\left|\psi^3 - \frac{4}{h_1}\left(b\psi^2 + \frac{1}{2}\beta\psi + \frac{1}{3}\gamma\right)\right| = (\psi_1 - \psi)\sqrt{\psi - \psi_m},$$

with $\psi_m < \psi < \psi_1$. Thus, one obtains the following solitary wave solution:

$$\psi(\xi) = \psi_1 - (\psi_1 - \psi_m)\mathrm{sech}^2\left(\frac{1}{2}\sqrt{h_1(\psi_1 - \psi_m)}\xi\right). \tag{4.5}$$

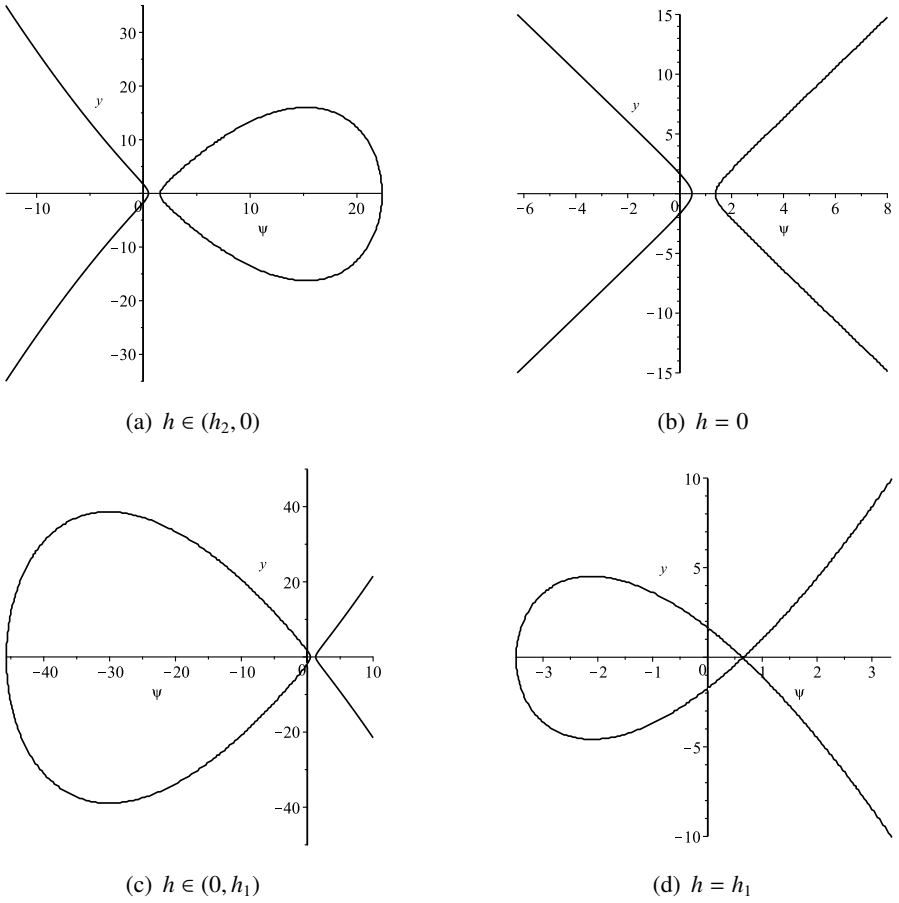

(a) $h \in (h_2, 0)$ (b) $h = 0$

(c) $h \in (0, h_1)$ (d) $h = h_1$

Figure 4. The level curves given by $H(\psi, y) = h$ of system (2.1) in Figure 2(c).

4.4. The case of $b > 0, \gamma < 0, h_1 < 0 < h_2$illustrated in Figure 2(d)

In this case, the changes of the level curves given by $H(\psi, y) = h$ are displayed in Figure 5.

(i) Corresponding to the homoclinic orbit to the singular point $E_1(\psi_1, 0)$ given by $H(\psi, y) = h_1$ in Figure 5(a), passing through the singular straight line $\psi = 0$ at $S_{\mp}$, it has the same parametric representation as (4.4).

(ii) Considering the periodic orbit family defined by $H(\psi, y) = h, h \in (h_1, 0)$ in Figure 5(b), which intersects the singular straight line $\psi = 0$ at $S_{\mp}$, it has the same parametric representation as (4.2).

(iii) Considering the periodic orbit family defined by $H(\psi, y) = 0$ in Figure 5(c), which intersects the singular straight line $\psi = 0$ at $S_{\mp}$, it has the same parametric representation as (3.2).

(iv) Corresponding to the periodic orbit family given by $H(\psi, y) = h, h \in (0, h_2)$ in Figure 5(d), passing through the singular straight line $\psi = 0$ at $S_{\mp}$, it has the same parametric representation as (4.3).

(v) Corresponding to the homoclinic orbit to the singular point $E_2(\psi_2, 0)$ given by $H(\psi, y) = h_2$ in Figure 5 (e), passing through the singular straight line $\psi = 0$ at $S_{\mp}$, now, (4.1) can be written as

$$\sqrt{h_2}\xi = \int_{\psi_m}^{\psi} \frac{d\psi}{(\psi_2 - \psi)\sqrt{\psi - \psi_m}},$$

where ψ_m is determined by

$$\left|\psi^3 - \frac{4}{h_2}\left(b\psi^2 + \frac{1}{2}\beta\psi + \frac{1}{3}\gamma\right)\right| = (\psi_2 - \psi)\sqrt{\psi - \psi_m},$$

with $\psi_m < \psi < \psi_2$. Thus, we have the following solitary wave solution

$$\psi(\xi) = \psi_2 - (\psi_2 - \psi_m)\text{sech}^2\left(\frac{1}{2}\sqrt{h_2(\psi_2 - \psi_m)}\xi\right). \tag{4.6}$$

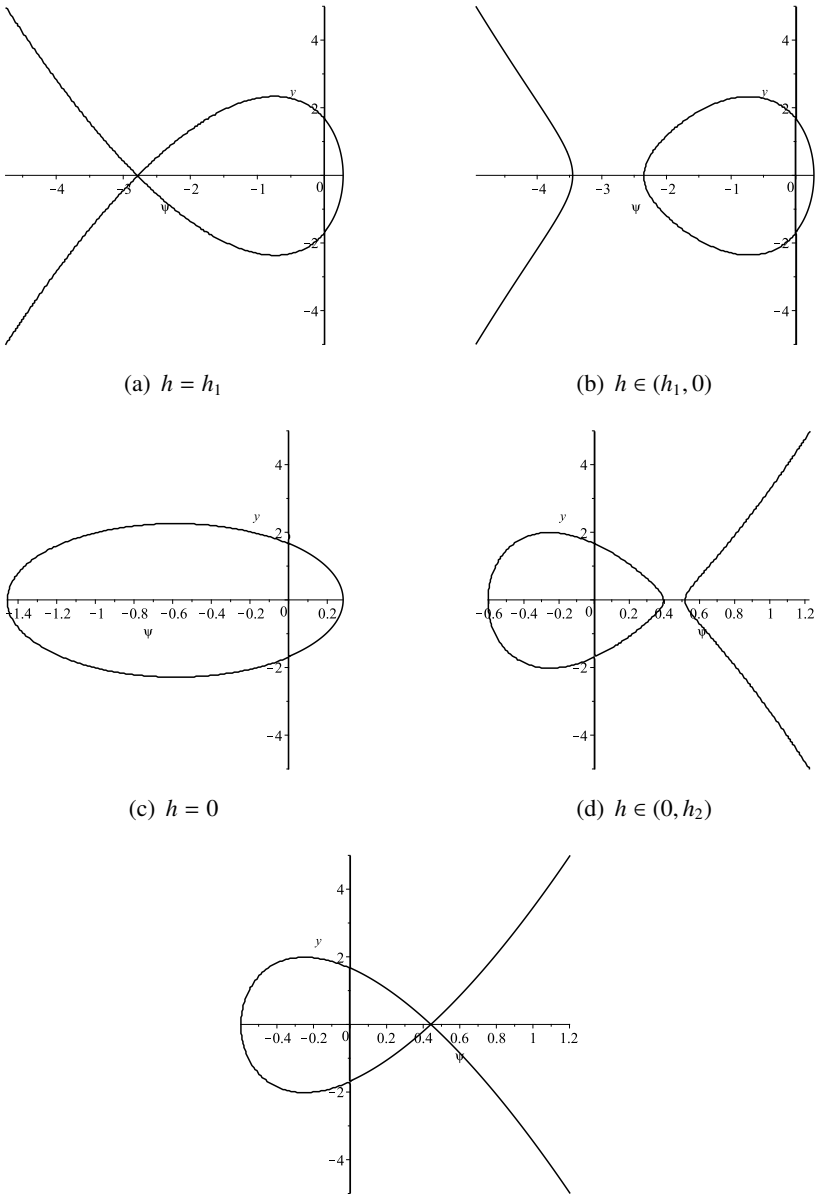

(a) $h = h_1$ (b) $h \in (h_1, 0)$

(c) $h = 0$ (d) $h \in (0, h_2)$

(e) $h = h_2$

Figure 5. The level curves given by $H(\psi, y) = h$ of system (2.1) in Figure 2(d).

5. Conclusions

In summary, this paper provides a comprehensive analysis of the generalized nonlinear Schrödinger equation by transforming it into a planar dynamical system. We identified several distinct parametric representations for the solutions, including solitary waves, periodic waves, peakons, and periodic peakons. These findings not only enrich the theoretical framework of nonlinear wave propagation but also offer practical guidance for designing optical systems with tailored wave characteristics. Future work will focus on extending this analysis to more complex nonlinear models and exploring their applications in other physical systems.

We will list the main conclusions as follows.

Theorem 1. (1) *For the generalized nonlinear Schrödinger equation (1.1), to find the exact explicit solutions with the form* $q(x,t) = (\psi(\xi))^{-\frac{1}{n}} e^{i(\kappa x-\omega t)}$, $\xi = x-2\kappa t$, *the amplitude component* $\phi(\xi) = (\psi(\xi))^{-\frac{1}{n}}$ *satisfies the planar dynamical system (1.11) with respect to* $\psi(\xi)$ *and has the first integral (1.12).*

(2) *Assume that* $\delta = \lambda = 0$ *and* $n = -\frac{1}{3}, n = 2$, *respectively. Under different parametric conditions, system (1.11) has the bifurcations of phase portraits, which are shown in Figures 1 and 2.*

(3) *For* $n = -\frac{1}{3}, n = 2$, *system (1.11) has 8 exact explicit parametric representations given by (3.2)–(3.5), and (4.2)–(4.5). The homoclinic orbits give rise to solitary wave solutions of Eq (1.11) with the parametric representations given by (3.5), (4.4), and (4.5). For* $n = 2$, *the periodic orbit families give rise to periodic wave solutions of Eq (1.11) with the parametric representations (4.2) and (4.3).*

(4) *Specially, when* $n = -\frac{1}{3}$, *system (1.11) has a periodic solution, a periodic peakon solution, and an anti-peakon solution with parametric representations given by (3.2), (3.3), and (3.4).*

Author contributions

Qian Zhang: Writing-original draft, Conceptualization, Data curation, Formal analysis; Ai Ke: Writing-review & editing, Methodology, Software, Validation. All authors have read and approved the final version of the manuscript for publication.

Use of Generative-AI tools declaration

The authors declare they have not used Artificial Intelligence (AI) tools in the creation of this article.

Acknowledgments

The first author is supported by the Sichuan Science and Technology Program (Grant No. 2024NSFSC1396) and the National Natural Science Foundation of China (12401241). The second author is supported by the National Natural Science Foundation of China (12301214).

Conflict of interest

The authors declare that they have no conflict of interest.

References

1. A. H. Arnous, A. Biswas, M. Ekici, A. K. Alzahrani, M. R. Belic, Optical solitons and conservation laws of Kudryashov's equation with improved modified extended tanh-function, *Optik*, **225** (2021), 165406. https://doi.org/10.1016/j.ijleo.2020.165406
2. A. Biswas, A. Sonmezoglu, M. Ekici, A. K. Alzahrani, M. R. Belic, Cubic-quartic optical solitons with differential group delay for Kudryashov's model by extended trial function, *J. Commun. Technol. Electron.*, **65** (2020), 1384–1398. https://doi.org/10.1134/S1064226920120037
3. P. F. Byrd, M. D. Fridman, *Handbook of elliptic integrals for engineers and scientists*, Berlin: Springer, 1971. https://doi.org/10.1007/978-3-642-65138-0
4. M. Ekici, A. Sonmezoglu, A. Biswas, Stationary optical solitons with Kudryashov's laws of refractive index, *Chaos Soliton. Fract.*, **151** (2021), 111226. https://doi.org/10.1016/j.chaos.2021.111226
5. N. M. Elsonbaty, N. M. Badra, H. M. Ahmed, S. Alkhatib, A. M. Elsherbeny, New visions of optical soliton to a class of generalized nonlinear Schrödinger equation with triple refractive index and non-local nonlinearity, *Ain Shams Eng. J.*, **15** (2024), 102641. https://doi.org/10.1016/j.asej.2024.102641
6. M. S. Ghayad, N. M. Badra, H. M. Ahmed, W. B. Rabie, Derivation of optical solitons and other solutions fornonlinear Schrödinger equation using modifed extended direct algebraic method, *Alex. Eng. J.*, **64** (2023), 801–811. https://doi.org/10.1016/j.aej.2022.10.054
7. A.-A. Hyder, A. H. Soliman, An extended Kudryashov technique for solving stochastic nonlinear models with generalized comformable derivatives, *Commun. Nonlinear Sci.*, **97** (2021), 105730. https://doi.org/10.1016/j.cnsns.2021.105730
8. A.-A. Hyder, A. H. Soliman, Exact solutions of space-time local fractal nonlinear evolution equations generalized comformable derivative approach, *Results Phys.*, **17** (2020), 103135. https://doi.org/10.1016/j.rinp.2020.103135
9. N. A. Kudryashov, A generalized model for description of propagation pulses in optical fiber, *Optik*, **189** (2019), 42–52. https://doi.org/10.1016/j.ijleo.2019.05.069
10. N. A. Kudryashov, Implicit solitary waves for one of the generalized nonlinear schrödinger equations, *Mathematics*, **9** (2021), 3024. https://doi.org/10.3390/math9233024
11. N. A. Kudryashov, Model of propagation pulses in an optical fiber with a new law of refractive indices, *Optik*, **248** (2021), 168160. https://doi.org/10.1016/j.ijleo.2021.168160
12. N. A. Kudryashov, Optical solitons of the resonant nonlinear schrödinger equation with arbitrary index, *Optik*, **235** (2021), 166626. https://doi.org/10.1016/j.ijleo.2021.166626
13. N. A. Kudryashov, Solitary wave solutions of hierarchy with non-local nonlinearity, *Appl. Math. Lett.*, **103** (2020), 106155. https://doi.org/10.1016/j.aml.2019.106155
14. J. B. Li, *Singular nonlinear traveling wave equations: bifurcations and exact solutions*, Beijing: Science Press, 2013.
15. J. B. Li, G. R. Chen, On a class of singular nonlinear traveling wave equations, *Int. J. Bifurcat. Chaos*, **17** (2007), 4049–4065. https://doi.org/10.1142/s0218127407019858

16. J. B. Li, M. Han, A. Ke, Bifurcations and exact traveling wave solutions of the Khorbatly's geophysical Boussinesq system, *J. Math. Anal. Appl.*, **537** (2024), 128263. https://doi.org/10.1016/j.jmaa.2024.128263
17. N. Ozdemir, A. Secer, M. Ozisik, M. Bayram, Optical soliton solutions of the nonlinear Schrödinger equation in the presence of chromatic dispersion with cubic-quintic-septic-nonicnonlinearities, *Phys. Scr.*, **98** (2023), 115223. https://doi.org/10.1088/1402-4896/acff50
18. C. Rogers, G. Saccomandi, L. Vergori, Helmholtz-type solitary wave solutions in nonlinear elastodynamics, *Ric. Mat.*, **69** (2020), 327–341. https://doi.org/10.1007/s11587-019-00464-w
19. M. Wang, Y.-F. Yang, Degenerate solitons in a generalized nonlinear Schrödinger equation, *Nonlinear Dyn.*, **112** (2024), 3763–3769. https://doi.org/10.1007/s11071-023-09207-x
20. Y. Yildirim, A. Biswas, M. Ekici, O. Gonzalez-Gaxiola, S. Khan, H. Triki, et al., Optical solitons with Kudryashov's model by a range of integration norms, *Chinese J. Phys.*, **66** (2020), 660–672. https://doi.org/10.1016/j.cjph.2020.06.005
21. Y. Yildirim, A. Biswas, A. Kara, M. Ekici, A. K. Alzahrani, M. R. Belic, Cubic-quartic optical soliton perturbation and conservation laws with generalized Kudryashov's form of refractive index, *Chaos Soliton. Fract.*, **50** (2021), 354–360. https://doi.org/10.1007/s12596-021-00681-3
22. E. M. E. Zayed, R. M. A. Shohib, A. Biswas, M. Ekici, L. Moraru, A. K. Alzahrani, et al., Optical solitons with differential group delay for Kudryashov's model by the auxiliary equation mapping method, *Chinese J. Phys.*, **67** (2020), 631–645. https://doi.org/10.1016/j.cjph.2020.08.022
23. E. M. E. Zayed, R. M. A. Shohib, M. E. M. Alngar, A. Biswas, M. Asma, M. Ekici, et al., Solitons in magneto-optic waveguides with dual-power law nonlinearity, *Phys. Lett. A*, **384** (2020), 126697. https://doi.org/10.1016/j.physleta.2020.126697
24. E. M. E. Zayed, R. M. A. Shohib, M. E. M. Alngar, A. Biswas, A. H. Kara, A. Dakova, et al., Solitons and conservation laws in magneto-optic waveguides with generalized Kudryashov's equation by the unified auxiliary equation approach, *Optik*, **245** (2021), 167694. https://doi.org/10.1016/j.ijleo.2021.167694
25. J. S. Zhuang, Y. Zhou, J. B. Li, Bifurcations and exact solutions of the Gerdjikov-Ivanov equation, *Journal of Nonlinear Modeling and Analysis*, **5** (2023), 549–564. https://doi.org/10.12150/jnma.2023.549
26. E. M. E. Zayed, M. E. M. Alngar, A. Biswas, M. Asma, M. Ekici, A. K. Alzahrani, et al., Solitons in magneto-optic waveguides with Kudryashov's law of refractive index, *Chaos Soliton. Fract.*, **140** (2020), 110129. https://doi.org/10.1016/j.chaos.2020.110129
27. Y. Zhou, J. S. Zhuang, J. B. Li, Bifurcations and exact traveling wave solutions in two nonlinear wave systems, *Int. J. Bifurcat. Chaos*, **31** (2021), 2150093. https://doi.org/10.1142/s0218127421500930

AIMS Press